THE ASTROPHYSICAL JOURNAL, 202:165–182, 1975 November 15

ULTRAVIOLET OBSERVATIONS OF COOL STARS. III. CHROMOSPHERIC AND CORONAL LINES IN α TAURI, β GEMINORUM, AND α BOOTIS

W. MCCLINTOCK
Department of Physics, The Johns Hopkins University

JEFFREY L. LINSKY*†
Joint Institute for Laboratory Astrophysics, National Bureau of Standards and University of Colorado

R. C. HENRY*‡ AND H. W. MOOS*
Department of Physics, The Johns Hopkins University

AND

H. GEROLA
Joint Institute for Laboratory Astrophysics, University of Colorado and National Bureau of Standards
Received 1975 February 24; revised 1975 May 12

ABSTRACT

The ultraviolet spectrometer of the Princeton Experiment Package aboard the *Copernicus* satellite has been used to obtain high-resolution measurements of Lα, the Mg II λ2800 doublet, and upper limits on the Si III λ1206 line in the K giants α Tau and β Gem. The intensities and line shapes are compared with earlier observations of α Boo. The Lα and Mg II profiles for α Tau resemble those for α Boo, in that they are highly asymmetrical, while β Gem shows much more symmetrical profiles. The asymmetries for all lines except for those of α Boo and the Mg II lines of α Tau could be due to interstellar absorption. In the case of β Gem only, the O V intercombination line at 1218 Å is observed, suggesting a well-developed corona substantially cooler than that of the Sun. The Lα profiles of α Tau and β Gem are consistent with the low interstellar hydrogen abundance in the solar neighborhood previously obtained from a similar observation of the α Boo Lα profile. The strength of the Mg II λ2796 line can be used to measure transition region and coronal pressures, and indicates a decrease in both with later spectral type and/or increasing luminosity.

Subject headings: chromospheres, stellar — coronae, stellar — late-type stars — spectra, ultraviolet

I. INTRODUCTION

In a previous paper (Moos *et al.* 1974, Paper I) we presented *Copernicus* observations of the H I λ1216 (Lα) and Mg II λλ2795.5, 2802.7 lines in the K giant star α Boo (Arcturus). We present here new observations in our continuing study of the chromospheres and coronae of late-type stars. These observations include the Lα and Mg II lines mentioned above, upper limits on the Si III λ1206 and H I λ1026 (Lβ) lines for α Tau (Aldebaran), β Gem (Pollux), and α Boo, upper limits on the O V λ1218 intercombination line for α Tau and α Boo, and detection of the O V line in β Gem. Some of these results have been reported briefly elsewhere (McClintock *et al.* 1974; Gerola *et al.* 1974, Paper II).

Studies of the Ca II H and K line emission profiles (e.g., Liller 1968) show that α Tau and β Gem, in common with probably most other K giants, have chromospheric outer atmospheres. The detailed physical structure of such chromospheres is not known, however, and only a very few model stellar chromospheres have been computed such as those for α CMi (Ayres *et al.* 1974) and α Boo (Ayres and Linsky 1973, 1975; Simon 1970). One aim of the present series of observations is to provide a basis for the computation of better model chromospheres.

In the ultraviolet, low-spectral-resolution observations for these stars have been obtained for the Mg II doublet at 2800 Å by Doherty (1972) using the Wisconsin experiment on OAO-2. Also, Kondo (1972) obtained a 7 Å resolution spectrum of α Boo from a rocket as well as 0.25 Å resolution measurements of the Mg II doublet in α Tau from a balloon (Kondo *et al.* 1975). Low-resolution measurements of Lα and O I λ1304 for α Boo have been made using a rocket-borne instrument (Moos and Rottman 1972). No high-resolution far-ultraviolet observations for α Tau or β Gem have been previously obtained to our knowledge.

* Guest Investigator with the Princeton University telescope on the *Copernicus* satellite, which is sponsored and operated by the National Aeronautics and Space Administration.

† Staff member, Laboratory Astrophysics Division, National Bureau of Standards.

‡ Alfred P. Sloan Foundation Research Fellow.

TABLE 1

CHARACTERISTICS OF STARS OBSERVED

Parameter	β Gem	α Boo	α Tau	Reference
Spectral Type	K0 III	K2 IIIp	K5 III	Hoffleit 1964
$B - V$	1.00	1.23	1.53	Hoffleit 1964
$T_{\rm eff}$	4750	4160	3780	Johnson 1964
	4680	4030		Gustafsson *et al.* 1974
log g	2.8	1.7	1.8	Johnson 1964
	2.9	1.9		Gustafsson *et al.* 1974
$L/L_\odot$	34	134	366	Conti *et al.* 1967
Distance (pc)	10.8	11.1	20.8	Hoffleit 1964
$R/R_\odot$	11.3	16	61	Wesselink 1969
		24	45	Pease 1931
		26		Gezari *et al.* 1972
[Fe/H]	−0.01	−0.51		Gustafsson *et al.* 1974
$A_\odot/A$	1	3	1	Conti *et al.* 1967
Ca II INT	1	2	4	Wilson and Bappu 1957
Ca II W (km s^{-1})	58	65	71	Wilson and Bappu 1957
W_{10830} (mÅ)	140	0	0	Vaughan and Zirin 1968

Although α Tau, β Gem, and α Boo are all K-type giants, they are three quite different stars. In particular (see Table 1), their effective temperatures, surface gravities, luminosities, and metal abundances all differ. Also, only β Gem exhibits He I λ10830 absorption (Vaughan and Zirin 1968), suggesting that its chromosphere may differ qualitatively from those of α Boo and α Tau.

The present observations were obtained in a study originally directed toward stellar chromospheres, but an exceptionally interesting result is the detection of the O V intercombination ($2s^2\ ^1S_0$–$2s2p\ ^3P_1^o$) line at 1218.406 Å in the star β Gem. In Paper II we have investigated the question of whether the O V line is formed in an analog of the solar chromosphere-corona transition region, or in an analog of the solar corona itself, and concluded that the line is probably formed in a true corona.

Analogs of several phenomena and structures in the solar outer atmosphere such as chromospheres, flares, and winds have not been seen in late-type stars. Although the coronal lines λ6374 of [Fe X] and λ5303 of [Fe XIV] are seen in late stages of such novae as CP Pup and Nova Her 1960, and additional coronal lines are often seen in recurrent novae (Joy 1961*a*; McLaughlin 1961), no spectroscopic or other direct evidence of late-type stellar *coronae* has been obtained for non-exploding stars until now. Even for flare stars such as UV Cet, U Gem, and Z Cam (Joy 1961*b*) the highest stage of ionization seen is He II (λ4686), which is indicative of chromospheric rather than coronal conditions. Centimeter radio emission has been detected from such stars as T Tau and LkHα 101 (Spencer and Schwartz 1974) and α Sco (Wade and Hjellming 1971; Oster 1971), but from these data it is difficult to determine an electron temperature in the emitting region and thus determine whether a corona is responsible. In any case, the emission from α Sco comes from the B3 V companion, and not from the red supergiant (Hjellming and Wade 1971).

In § II we present the *Copernicus* observations on which this paper is based and discuss corrections for the particle-induced background noise. The line shapes, evidence regarding variability, and absolute intensities are discussed in § III, together with a discussion of the Mg II k/h line ratios, and upper limits on the local interstellar hydrogen density and their implications for the interstellar medium. Finally in § IV we derive possible transition region and coronal models for these stars and consider what range of parameters the data suggest.

II. OBSERVATIONS

Low-resolution (~0.2 Å) measurements with the *Copernicus* spectrometer (Rogerson *et al.* 1973*a*) were made on 1973 February 5/6 and 1973 October 17/18 for α Tau, and on 1973 October 16/17 for β Gem. A summary of these observations is given in Table 2. Also included for comparison are the α Boo measurements made on 1973 May 19/20, that were discussed in Paper I. The first observation of α Tau was exploratory in nature and was the first *Copernicus* observation of a late-type star.

The spectrometer has a fixed grating, and spectral scanning is accomplished by moving the exit slit and its detector in discrete steps along the exit plane. Each motion of the carriage is preceded by a 14-s integration period during which time the exit slit and detector remain stationary. The step size (0.174 Å at Lα and 0.323 Å at Mg II) is slightly smaller than the nominal exit slit width (0.185 Å at Lα and 0.397 Å at Mg II). Because of the weakness of the stellar signal it was necessary to average several scans in order to obtain a useful signal-to-noise ratio. The number of scans that were averaged, and the total dwell time per spectral step are given in Table 2 for each data set. Reduction of low-signal-level data from *Copernicus* is complicated by the presence of a substantial background (due primarily to trapped terrestrial particles, and cosmic rays) and to a lesser extent by Doppler shifts in the wavelength scale introduced by the orbital motion of the spacecraft.

For the October observations, the spectrometer was programmed to step toward longer wavelengths for 40 consecutive steps and then to reverse direction and

TABLE 2

SUMMARY OF RESULTS

	α Tau (K5 III) 1973 Feb. 5/6	α Tau (K5 III) 1973 Oct. 15/16	α Boo (K2 III) 1973 May 19/20	β Gem (K0 III) 1973 Oct. 16/17	Sun (G2 V)	
Lα λ1215.7:						
Number of spectral scans	4	16	8	14	...	
Total dwell time per step(s)	56	224	112	196	...	
Line counts per 14 s:						
Blue Component	44.5 ± 10.0	38.1 ± 5.5	90.6 ± 8.1	18.6 ± 5.6	...	
Red Component	76.3 ± 10.9	81.0 ± 8.3	165.6 ± 9.2	12.2 ± 5.3	...	
Total	120.8 ± 17.0	119.1 ± 11.1	256.1 ± 12.9	30.8 ± 8.4	...	
Flux observed (ph cm^{-2} s^{-1}):						
Blue Component	0.93	0.80	1.89	0.39	...	
Red Component	1.59	1.69	3.46	0.26	...	
Total	2.52	2.49	5.35	0.65	...	
Stellar surface flux* (10^3 ergs cm^{-2} s^{-1}):						
Blue Component	6.49	5.57	11.3	11.6	...	
Red Component	11.1	11.8	20.7	7.63	...	
Total	17.6	17.4	32.1	19.2	249.0 ± 37.0	(1)
Full width at half-intensity (Å)	...	2.6 ± 0.3	2.3 ± 0.2	1.4 ± 0.2	1.4 ± 0.3	(4)
O v λ1218.4 (upper limits in parentheses):						
Number of spectral scans	...	16	8	14	...	
Total dwell time per step(s)	...	224	112	196	...	
Line counts per 14 s	...	(10.5)	(15.6)	12.0 ± 4.0	...	
Flux observed (ph cm^{-2} s^{-1})	...	(0.22)	(0.33)	0.25	...	
Stellar surface flux (10^3 ergs cm^{-2} s^{-1})	...	(1.53)	(1.95)	7.50	0.3	(3)
Si III λ1206.5 (upper limits in parentheses):						
Number of spectral scans	...	12	24	12	...	
Total dwell time per step(s)	...	168	336	168	...	
Line counts per 14 s	...	(10.25)	(8.10)	(11.43)	...	
Flux observed (ph cm^{-2} s^{-1})	...	(0.22)	(0.17)	(0.25)	...	
Stellar surface flux (10^3 ergs cm^{-2} s^{-1})	...	(1.46)	(0.99)	(6.95)	1.96 ± 0.29	(1)
Mg II λ2795.5 and λ2802.7:						
Number of spectral scans	4	16	6	18	...	
Total dwell time per step(s)	56	224	84	252	...	
Line counts per 14 s:						
λ2796	4507 ± 863	3019 ± 563	12,927 ± 850	1297 ± 538	...	
λ2803	2909 ± 697	2187 ± 658	11,200 ± 750	1385 ± 337	...	
Flux observed (ph cm^{-2} s^{-1}):						
λ2796	14.0	9.41	40.2	4.04	...	
λ2803	9.1	6.81	34.9	4.32	...	
Stellar surface flux (10^3 ergs cm^{-2} s^{-1}):						
λ2796	41.7	27.9	103	51.3	650.0	(2)
λ2803	26.9	20.2	89	54.8	550.0	(2)
Full width at base (Å), λ2796	...	1.6:	1.6	1.0:	0.97	(2)
Lβ λ1025.7 (upper limits in parentheses):						
Number of spectral scans	...	2	28	2	...	
Total dwell time per step(s)	...	28	392	28	...	
Line counts per 14 s	...	(123)	(57)	(67)	...	
Flux observed (ph cm^{-2} s^{-1})	...	(0.93)	(0.33)	(0.50)	...	
Stellar surface flux (10^3 ergs cm^{-2} s^{-1})	...	(7.5)	(2.3)	(17)	3.1	(5)

* Not corrected for interstellar H I absorption.

REFERENCES.—(1) Rottman 1974. (2) Tousey *et al.* 1974. (3) Chipman 1974. (4) Tousey 1967. (5) Hall and Hinteregger 1970.

step toward shorter wavelengths for 40 consecutive steps. In this mode the wavelength positions of the steps for each scan are the same in the rest frame of the spectrometer. The February α Tau observations were programmed so that each scan overlapped the preceding scan by $\frac{1}{4}$ step. This technique is useful in obtaining increased spectral information for stars with large ultraviolet fluxes; however, in the case of low signal-to-noise ratios this procedure only complicates the analysis and interpretation of the data.

Table 2 summarizes all of the observational results for the stars α Tau, β Gem, and α Boo, including estimates of the stellar surface fluxes based on the distances and stellar radius data of Table 1.

a) H I λ*1216 Observations*

The solid line in Figure 1 is a histogram of the average of 16 scans of α Tau made 1973 October 17/18, after background subtraction. The dashed line is a similar histogram of the four scans made 1973 February 5/6. The background subtracted was determined from dark count data accumulated during several thousand orbits of the satellite. The dark count data have been averaged over four integration periods (1 "spacecraft minute") near a given magnetic latitude and longitude to produce an "estimated standard background," as a function of magnetic latitude and longitude. Because the data are averaged over four integration periods, use of this background suppresses the additional noise that would be introduced by using a real-time background monitor. The estimated standard background has proven successful for removing large slopes introduced into the data by the variation in trapped particles and cosmic rays with spacecraft position. There is evidence (York 1974*a*) that the particle background fluctuates in intensity as a function of time. Therefore, after subtracting the standard background and histogramming the data, a straight line was fitted by the method of least squares using the two spectral intervals away from Lα (1212.1 to 1214.0 Å, and 1217.8 to 1219.2 Å; 19 spectral steps) where no signal was expected. In the fitting, the residual values were weighted by the reciprocal of their variance as determined from the rms scatter of the average of 16 scans (October) or four scans (February). For the February data, two points having disproportionately high weights (due to statistical accident with this small number of scans) were deleted from the fit. This line, for each of the observations, is shown in Figure 1.

The resolution of the histogrammed October 17/18 observations is estimated to be 0.25 Å. Although the nominal exit slit width of the spectrometer is only 0.185 Å at Lα, the spacecraft orbital motion introduces small shifts in the wavelength scale from scan to scan of about 0.03 Å. Histogramming such scans introduces a smearing in wavelength (and therefore a reduction in resolution) of about 0.06 Å. Error bars in Figure 1 are $\pm 1\,\sigma$ errors, where σ is the error of the mean estimated from the rms scatter among 16 measurements at that wavelength.

Although the fluctuations in the stellar signal are probably best described by Poisson statistics, rms errors are used here to characterize the confidence in the data because two additional sources of noise contribute significantly to the total fluctuations in the data. The first arises from the fact that each photomultiplier counter has a precounter which scales the measured count rate. For the data presented here, the

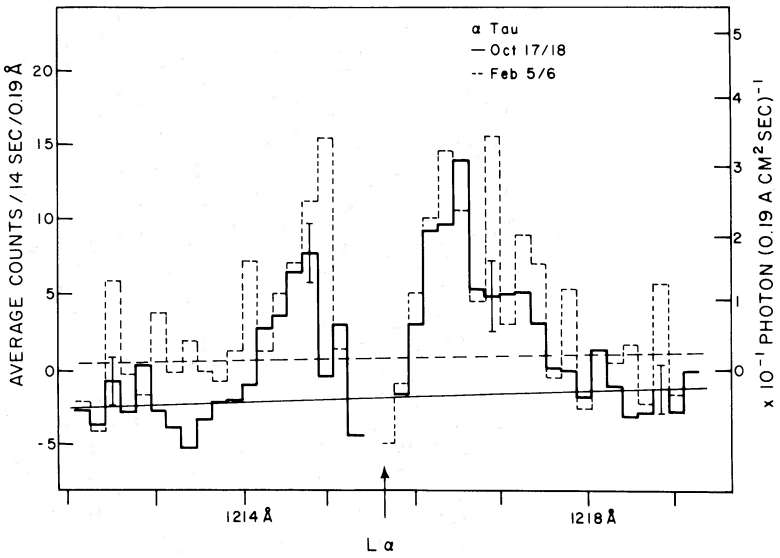

FIG. 1.—The solid histogram is the average of 16 spectral scans of the H I λ1216 Å emission from Aldebaran obtained 1973 October 17/18. The ordinate is the number of photomultiplier pulses per 14 s period, per resolution element. Errors in the mean are $\pm 1\,\sigma$ (rms). For comparison, the average of four spectral scans acquired 1973 February 5/6 are shown (*dashed histogram*). No error bars are shown. Within experimental error, there is no evidence for variability of the H I λ1216 emission on the time scale of 8.3 months. The line is strongly asymmetric, with a reversal due probably to a combination of intrinsic self-reversal, a stellar wind, and interstellar hydrogen absorption.

only serious effect is on the far-ultraviolet low-resolution detector, for which the prescale factor is 8. Although systematic analysis of scaled data is possible (Evans 1955), a second more serious source of fluctuation in the data comes from the particle- and cosmic-ray–induced background.

Unfortunately the nature of the statistical distribution that describes the background is not well known and may differ from Poisson statistics. Furthermore, the data from different spectral scans are acquired at very different geomagnetic locations (the Earth turns under the plane of the spacecraft orbit), which introduces additional uncertainties in determining the background. For the case where the ratio of particle background noise to stellar signal is almost always greater than unity, error estimates based on Poisson distributions (i.e., on the square root of the number of counts) may lead to incorrect conclusions. Therefore, although the rms error was always found to be very close to the error predicted by Poisson statistics, the more conservative approach (i.e., the use of the rms errors) has been adopted for analyzing these data.

The two steps at the center of the line, severely contaminated by geocoronal Lα emission, are deleted. The total Lα signal summed from 1214.0 to 1217.8 Å is 119.1 ± 11.1 counts per 14 s, relative to the least-squares-fit line.

As described above, the four scans obtained on February 5/6 are overlapped by ¼-step intervals. Histogramming these scans further degrades the resolution. It might be thought that this problem could be overcome by linearly interpolating between the points of individual scans and then averaging the interpolated spectra. However, where signal-to-noise ratios are small, linear interpolation can add fictitious structure to the individual scans. For this reason, the four scans were histogrammed after the background was removed by the procedure described above. For the February 5/6 observations the total Lα signal relative to the least-squares-fit line, summed over the same wavelength interval, is 120.8 ± 17.0 counts per 14 s.

The Lα observations of β Gem (Fig. 2) consist of 18 low-resolution scans. These data have been briefly described in Paper II and by McClintock *et al.* (1974). Reduction of the data from β Gem using the techniques described above gives somewhat unsatisfactory results, because the signal-to-noise ratio was only about 0.35 the signal-to-noise ratio for α Tau. It was therefore decided to use the high-resolution channel of the spectrometer as a real time background monitor. This also eliminated the possibility that unsuspected time-dependent background events might cause spurious spectral features. Independent testing has shown that the ratio of high-resolution detector dark count to low-resolution detector dark count is 1.30. The spectrometer had been programmed to simultaneously scan Lα at low resolution and Mg II (λ2795.5) with the near-ultraviolet high-resolution detector. In that configuration, the far-ultraviolet high-resolution detector scans a region of the spectrum 1297.2 to 1298.9 Å. Careful examination of the high-resolution spectrum revealed no emission lines present in this region; and since β Gem is spectral class K0 III, no detectable continuum emission is expected. Using these data as a monitor determines the real-time particle background for the low-resolution detector. However, this real-time background resulted in data somewhat noisier than was the case when an "average" background was subtracted, because only 15 s of data were used in determining the background.

Figure 2 is a histogrammed average of 14 scans of β Gem after background subtraction. We deleted three steps at the center of the line which are strongly contaminated by geocoronal Lα emission. The average background for the 18 scans varied between 16 and 54 counts per spectral step. We also deleted the four scans which had average background levels above 50 counts per spectral step. Neither constant of a least-squares straight line fit to the residuals away from Lα and excluding the region 1218.0 to 1218.8 Å was statis-

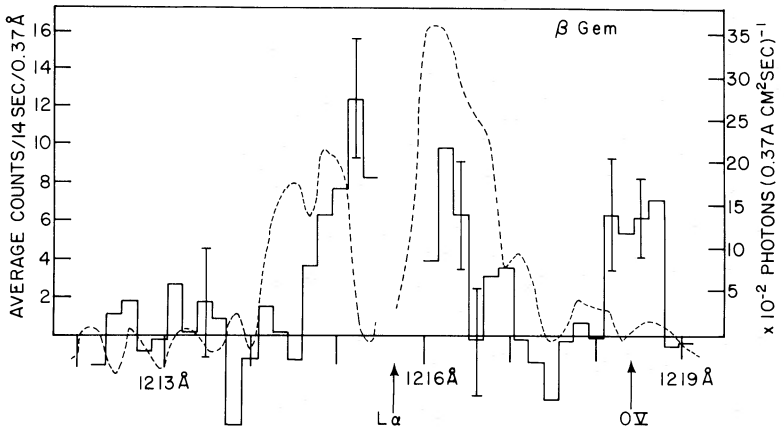

FIG. 2.—The average of 14 spectral scans of the Lα region of β Gem is shown (*solid histogram*) compared with scans for α Boo (Moos *et al.* 1974), reduced in intensity by a factor of 3.9 (*dashed line*). A strong feature, present in the β Gem spectrum at 1218.4 Å but absent from the Arcturus spectrum, is identified as a coronal emission line of O v. Arrows indicate nominal Lα and O v wavelengths. The β Gem Lα profile shows no evidence for a stellar wind.

tically significant, indicating that this background subtraction technique is highly reliable. The reliability of the baseline has been estimated to be ± 0.41 counts per 14 s from the scatter of the 19 spectral elements used in determining it about an assumed mean of zero. Finally the data were degraded in resolution to 0.4 Å by summing the counts in pairs of adjacent spectral steps. Thus the count rate shown at each discrete data point is the *sum* of two independent measurements at 0.087 Å on either side of the histogram bar. This technique gives a resolution equivalent to using an exit slit which is twice as wide as the actual exit slit, although it should be noted that only every second point contains completely independent data. The error bars are $\pm 1\ \sigma$, where σ as before is the error of the mean estimated from the rms scatter among the 14 measurements at that wavelength.

Figure 2 clearly demonstrates the presence of Lα emission from β Gem. (For comparison, the Arcturus Lα profile of Paper I, reduced a factor 3.9, is also shown.) The total Lα signal summed from 1214.6 to 1217.1 Å is 30.8 ± 8.4 counts per 14-s integration period.

b) O v λ*1218 Observations*

In addition to the β Gem Lα signal in Figure 2, an emission feature appears at 1218.35 ± 0.10 Å. The integrated strength of this feature is 12.0 ± 4.0 counts per 14-s integration period, i.e., about 0.38 the integrated strength of the stellar Lα signal. In Paper II we argued that this feature is real and identified it as the O v intercombination line ($^1S_0$–$^3P_1^o$) at 1218.406 Å, originating in a cool corona in this star.

Neither the α Boo spectrum in Figure 2, nor the α Tau observations in Figure 1, show evidence for a stellar O v line, but 3 σ upper limits can be set using the method discussed in § II*d*. These upper limits are given in Table 2.

c) Mg II λ*2796 and* λ*2803 Observations*

Low-resolution (~ 0.51 Å) scans of the Mg II resonance lines at 2800 Å were obtained using programs identical to those used for the Lα observations. The background subtraction procedure for the near-ultraviolet detectors is complicated by the fact that these detectors are more sensitive to trapped terrestrial particles than are the far-ultraviolet detectors. Backgrounds estimated from dark-count data are available, and it was possible to gain some insight into the reliability of these estimates by comparing the prediction of the "standard background" with actual dark-count data that were acquired during the orbits in which the Mg II scans were made. For both α Tau and β Gem the observed background is about 1.5 times the standard background. Furthermore, for the β Gem observations which extended over 10 orbits the fluctuations from orbit to orbit in the ratio of observed to predicted dark count were found to be about 10 percent.

The solid line in Figure 3 is a histogrammed average of 16 scans of α Tau obtained October 17/18, after background subtraction. The dashed line is a similar histogram of four scans obtained February 5/6. For both sets of data the standard background was normalized by using the average ratio of observed to predicted dark counts for the orbits during which Mg II scans were made. The solid straight line is a least-squares fit to the October data excluding the regions 2794.7 to 2796.6 Å and 2801.8 to 2803.7 Å. The slope of this baseline, which is not significantly different from zero, is not affected by small changes in the normalization factor used to correct the standard background; however, the constant coefficient in the least-squares fit changes by about 300 counts per 14 s for only a 6 percent error in the normalization factor. Thus the absolute count rates are uncertain, and the zero level in Figure 3 is arbitrary. Error bars are $\pm 1\ \sigma$, where σ has the same meaning as before.

As described above, the four scans obtained on February 5/6 are overlapped by $\frac{1}{4}$-step intervals. These scans were histogrammed in the same manner as the Lα observations, with the result that the resolution is slightly degraded. The data were treated in the same manner as the October observations. In computing the baseline, one point of disproportionately high weight has been discarded. The Mg II emission for both observations was summed relative to its respective least-squares-fit baseline, and the result is given in Table 2.

Interpretation of the details of the spectra is complicated by the extreme noise in the data. A vital parameter for the discussion of line profiles is the wavelength calibration of the spectrometer. If nominal line center is truly represented by the arrows in Figure 3, the existence of striking asymmetry in the λ2795.5 (*k*) line is beyond question. The two spectral steps longward of line center are 8 σ and 4.5 σ above the least-squares-fit baseline, while the spectral steps shortward of line center are 0.8 σ and 1.4 σ above the baseline. Although emission is clearly present in only three spectral steps, the possibility that there is *no* emission shortward of nominal line center is highly unlikely, and therefore emission appears in at least five spectral steps (even though it may be nearly buried in the noise for the two shortward steps). That the λ2802.7 line is also broad is then deduced from the fact that both lines are formed at nearly the same temperature (and therefore height) in the stellar chromosphere, and the fact that the width of the *k* line is only slightly greater than the width of the *h* line in other stars (e.g., α Boo, α Ori, and the Sun). However, the shape of the *h* line *could* be different from the *k* line, as in the case of α Ori. On the other hand, if the true nominal line center were actually one spectral step longward from its position as marked in the figure, then the data are so noisy that no conclusion that asymmetry is present would be possible, and a strict interpretation would be that the *k* and *h* lines are narrow (~ 3 spectral steps), redshifted, and symmetric.

T. Snow (private communication) informs us that the wavelength scale of the spectrometer is reliable to better than $\pm\frac{1}{2}$ step (0.2 Å at λ2800 Å or 20 km s^{-1}). The change of 34 km s^{-1} in radial velocity (from an assumed nominal value of $+54$ km s^{-1}) required to

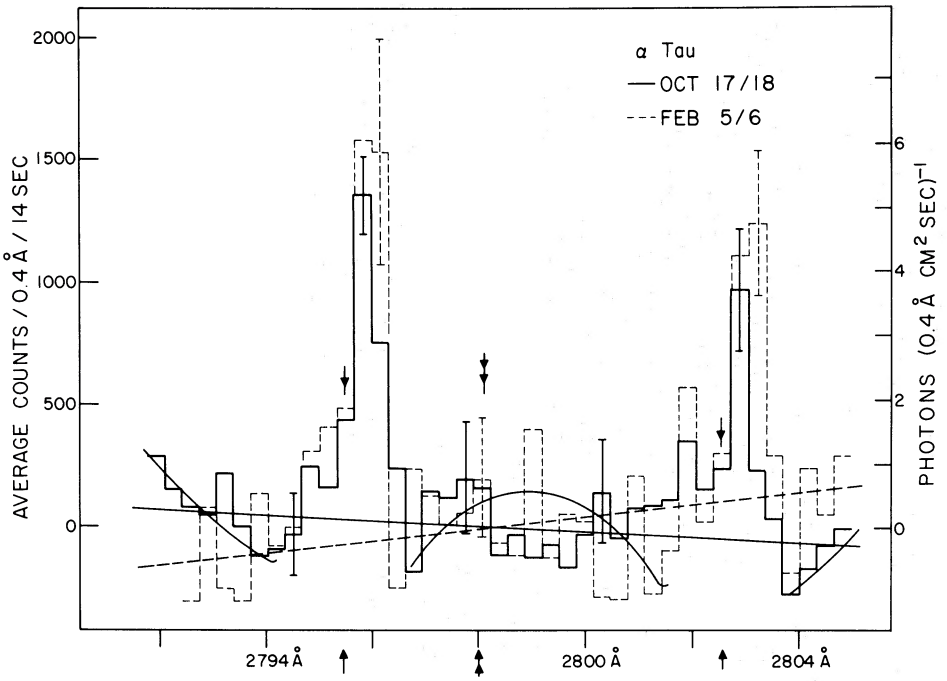

FIG. 3.—Observed Mg II emission from Aldebaran on 1973 October 17/18 is shown as a heavy solid histogram. Single-headed arrows indicate nominal line centers at 2795.5 and 2802.7 Å. The smooth curve represents the shape of the solar Mg II absorption lines at 2800 Å (Tousey *et al.* 1974). Double-headed arrows show the wavelength position of one component of the subordinate transition ($3p\ ^2P^o$–$3d\ ^2D$) of Mg II. For comparison four scans acquired February 5/6 are also shown (*dashed histogram*). All error bars are $\pm 1\ \sigma$ (rms).

produce such a wavelength shift has not been observed in extended studies of the Ca II K line of this star (Deutsch 1970). Furthermore, recent observations by Kondo *et al.* (1975) clearly demonstrate that the Mg II *k* line is both asymmetric and broad. Therefore, although this second interpretation cannot be *totally* refuted by the data presented here, there can be little doubt that the first interpretation is correct.

It is possible that there is no detected *photospheric* emission at these wavelengths and the linear baselines simply represent a very noisy zero-flux level. In the Sun, the Mg II resonance emission features are formed in the cores of the extremely deep and broad photospheric Mg II absorption lines. With sufficient sensitivity one might expect to see a sharp rise in the emission at both ends of the α Tau scan and a broad low-intensity emission between the cores of the lines. If the absorption lines are very broad and the upper photospheres cool as expected, the region between the two cores will be essentially flat (zero), and the least-squares line drawn in Figure 3 represents the best estimate of the baseline. For reference the shape of the solar Mg II absorption lines (Tousey *et al.* 1974) is represented in Figure 3 by a curved line. No clear evidence for such structure appears in the data.

Figure 4 is a histogrammed average of 18 scans of β Gem. As in the case of α Tau the straight line is a least-squares linear fit excluding the regions of Mg II emission (2794.7 to 2796.0 Å and 2802.1 to 2803.1 Å). It is obvious from Figure 4 that emission appears in three spectral steps for the *h* line, which implies that the *k* line should also show emission in at least three steps. Error bars are $\pm 1\ \sigma$. In this case the solid curve represents the shape of the solar continuum normalized to the strength of the Mg II *k* line (2795.75 Å).

For both α Tau and β Gem the data cannot confidently be used to decide whether the curved or straight baseline is appropriate, although the curved line for β Gem appears quite plausible. If the physical situation is represented by the curved baseline, then the total fluxes in Table 2 will be increased by about 1200 counts for the *h* and *k* lines of α Tau, 800 counts for the *k* line of β Gem, and 600 counts for the *h* line of β Gem.

In both figures single arrows mark the position of the nominal line center of Mg II *k* and *h*. Also shown (by a double arrow) is the position of the subordinate transition ($3p\ ^2P^o$–$3d\ ^2D$) of Mg II at 2798 Å. This line is present in the solar spectrum as a very weak absorption feature (Tousey *et al.* 1974).

d) Si III λ1206 *and* Lβ λ1026 *Observations*

The spectrometer program included 12 low-resolution scans of α Tau and β Gem and 24 scans of α Boo, in the spectral region 1203.0–1210.0 Å. Also included were 28 low-resolution scans of α Boo (1023.9–1027.5 Å), 10 high-resolution scans of α Boo (1025.3–1027.8 Å), and two high-resolution scans for α Tau and β Gem (1023.7–1027.8 Å). No emission was observed in the spectra of any of these stars for these wavelength regions. For those cases where a large number of

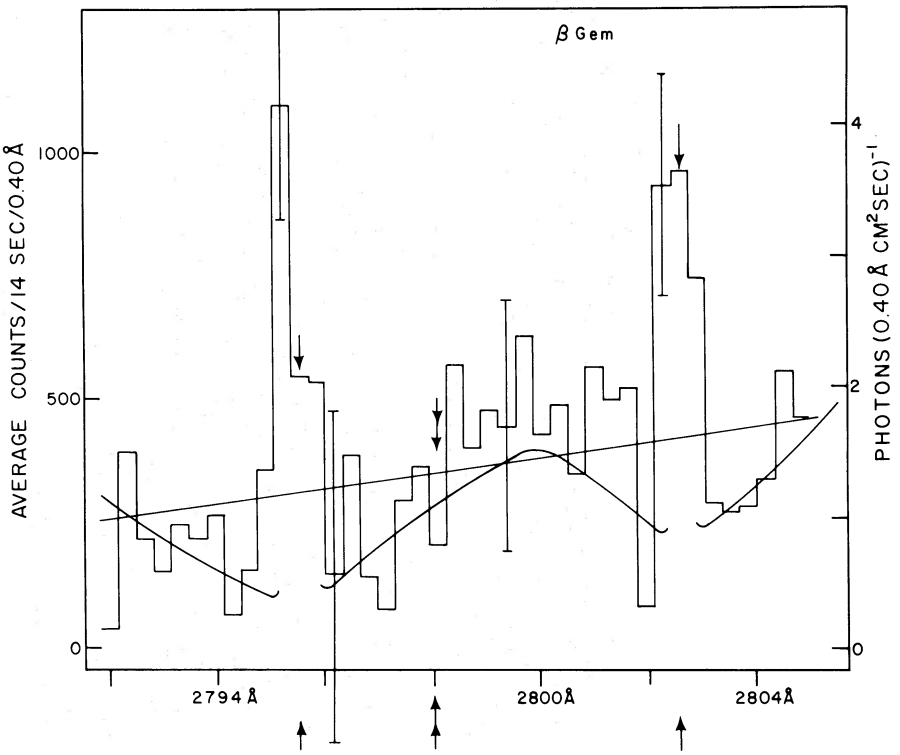

FIG. 4.—The average of 18 spectral scans of the Mg II region of β Gem. Single-headed arrows indicate nominal line centers at 2795.5 and 2802.7 Å. The smooth curve represents the observed shape of the solar Mg II absorption lines at 2800 Å normalized to the strength of the Mg II k line at 2795.5 Å. Double-headed arrows show the wavelength position of one component of the subordinate transition of Mg II as in Fig. 3.

scans (≥ 10) are summed to form an average spectrum, the rms scatter in the individual scans from the mean can be used to estimate the noise of the observation. Let σ_I represent the standard error in the mean of the individual scans for a single spectral step. Then 3 times σ_I gives a 3 σ upper limit for emission in that particular spectral step. For more than one step a 3 σ upper limit is given by

$$\left[\sum_{j=1}^{N} \sigma_j^2\right]^{1/2},$$

since the standard errors calculated for each spectral step are statistically independent.

Under the assumption that the 1206.5 Å line of Si III is about 1 Å wide (and therefore would appear in four adjacent spectral steps), Table 2 gives 3 σ upper limits for its strength summed over 0.8 Å wavelength band in counts per 14 s. Also given in Table 2 are upper limits for Lβ λ1025.7 emission from all three stars. In the Sun the Lβ line is $\sim$0.75 times the width of the Lα line (Tousey 1967). The Lβ width used for calculating upper limits was calculated by doubling the half-width (estimated as 0.75 Lα half-width in Table 2). For α Tau and β Gem only two scans were obtained, and considerable error may result from estimating σ_I from rms scatter: therefore, σ_I was also estimated from Poisson statistics. On the average, errors predicted by the two methods differed by only 10 percent. It was noted in § II*a* that the statistical distribution which describes the data is not completely known. Therefore, one should be cautious about the probability interpretations of a 3 σ upper limit which is based on a normal statistical distribution.

III. DISCUSSION OF THE OBSERVATIONS

Discussion of intrinsic stellar line shapes and absolute intensities requires that the observed profiles be corrected for interstellar absorption. A detailed discussion presented in §§ III*e* and III*f* confirms that the interstellar absorption has a small effect on the stellar Mg II line shape and total emission strength, while the observed total Lα emission strengths are strongly affected. Furthermore, the asymmetry in the α Tau Lα line shape discussed in the next paragraph may be strongly influenced by interstellar absorption, as discussed below.

a) Line Shapes

In Paper I we drew attention to the peculiar shape of the α Boo Mg II line profiles, which are characterized by a blueshifted central absorption feature and a longward emission peak much stronger than the shortward peak. The α Tau Mg II k profile also shows its peak emission longward of line center by about 0.20–0.25 Å, but the data are too noisy to show a weak shortward emission peak if present. The β Gem Mg II profiles are too noisy to show clearly any asymmetry.

We interpreted the asymmetric α Boo Mg II line profiles as indicating a stellar wind. The present data may suggest a similar wind for α Tau. The longward/shortward asymmetry seen in the α Boo Lα profile, which is also consistent with a "wind," is also seen in α Tau but not in β Gem. However, significant interstellar absorption (cf. § III*e*) could entirely account for the asymmetric α Tau Lα profile. A theoretical discussion of the origin of the Mg II asymmetrical profiles in an expanding stellar chromosphere is given by Linsky *et al.* (1974).

Paper I noted the interesting fact that the Lα and Mg II lines for α Boo are wide, compared to the same lines in the Sun. Included in Table 2 are estimates of the Lα full widths at half-intensity and the Mg II *k*-line full widths at the base corrected for instrumental broadening.

In the case of α Boo, limits on the Mg II widths were estimated by counting the number of spectral steps in which emission does appear. This establishes an upper limit on the width, while one step less on each side of the line clearly sets a lower limit. The difference between the upper and lower limits is unfortunately large, because the step size is such a significant fraction of the total line width. For α Tau and β Gem, this method produces only a lower limit, because the data are so noisy that the true line wings cannot be identified. Rigorous lower limits are three steps for α Tau and two steps for β Gem. The extremely uncertain best estimates given in Table 2 (five steps for α Tau and three steps for β Gem) were derived in the discussion of the Mg II line shapes in § II*c*.

In order to measure the Lα half-width, smooth curves were fitted to the histogrammed data by eye estimate. For α Boo and β Gem the widths measured from these curves need no correction for instrumental broadening since the intrinsic stellar width is much larger than the spectrometer resolution half-width, which is effectively 0.2 Å for α Boo and 0.4 Å β Gem. Uncertainties in the measured half-widths are estimated to be about 1 resolution element, which is small compared with the line width. Interpretation of the α Tau half-width is slightly ambiguous because the asymmetry in the profiles is pronounced. Using the entire profile to measure the full half-width leads to a value of 2.6 ± 0.3 Å.

b) Search for Variability in the α Tauri Emissions

There is evidence that the Ca II K line in α Tau is variable both in emission strength and in line shape. Liller (1968) finds variations of 20 percent in the strength of the individual shortward and longward components.

The two Lα observations for α Tau, made 8.3 months apart, are shown in Figure 1, and give no evidence for variability. The ratio of total signal for the October 17/18 observation to that of the February 5/6 observation, both summed from 1214.0 to 1217.8 Å, is 0.87 ± 0.14. The enhanced longward emission feature is present in both observations, and the ratio of shortward emission strength to longward emission strength is not significantly different (0.58 ± 0.13 for February 5/6 and 0.47 ± 0.07 for October 17/18). Recent measurements of the spectrometer efficiency indicate that the overall sensitivity of the instrument may have decreased by about 5 percent at 1200 Å between the two observations (Snow 1974). Within experimental error, therefore, there is no evidence for variation in either the profile or the total emission strength of Lα over this 8.3-month time interval.

The situation for Mg II is complicated by the very low signal-to-noise ratios. The ratio of total emission strength in the *k* line to that in the *h* line is not significantly different for the two α Tau observations (1.55 ± 0.44 for February 5/6 and 1.38 ± 0.42 for October 17/18). The ratio of $(k + h)$ for February to $(k + h)$ for October is 1.42 ± 0.35, which is not convincing evidence for variability. Observations of the B2 V star α Gru are available for the 10-month period 1972 November–1973 September, and indicate that the efficiency of the spectrometer at 2800 Å has not changed detectably. Thus, while the data do not indicate strong variability in the Mg II emission over a time interval of 8.3 months, further examination of this question would be profitable.

c) Absolute Intensities

The absolute efficiency of the spectrometer is not well known: the calibration factors in the far-ultraviolet (e.g., 0.00113 counts per photon on Lα) may be in error by as much as a factor of 2 (York 1974*a*). The absolute intensity of Lα for α Boo in Table 2 has been decreased nearly a factor of 2 from that reported in Paper I, using this latest revised calibration. The situation in the near-ultraviolet is even less satisfactory, and calibration is best accomplished by reference to the OAO-2 observations (Doherty 1972). This procedure was carried out for α Boo (Paper I) and from that result an efficiency of 0.0064 counts per photon for the low-resolution detector at 2800 Å can be inferred for 1973 May 19/20 (Snow 1974). This calibration procedure is based on the assumption that the Mg II flux from α Boo is not variable over long time intervals. Observations of α Gru made in 1972 November and 1973 September indicate no detectable change in spectrometer efficiency over a period of 10 months. Table 2 summarizes the absolute intensities for α Tau, β Gem, and α Boo.

The values of the stellar flux given in Table 2 have been computed using the distances in Table 1 and stellar radii of 11.3, 26, and 45 $R_\odot$ for β Gem, α Boo, and α Tau, respectively, with no correction for interstellar H I or Mg II absorption.

d) The Mg II *k/h Line Ratios*

It is expected that for an optically thick resonance doublet formed in a chromosphere where the temperature increases with height, the more opaque component will be formed slightly higher in the chromosphere and will therefore be slightly brighter. In the Sun the ratio of *k* emission to *h* emission is 1.18. For β Gem, α Boo, and α Tau (October observation) the ratios relative to the least-squares baselines are 0.94 ± 0.43,

1.15 ± 0.10, and 1.38 ± 0.42, respectively. The data are therefore consistent with the idea that the Mg II resonance lines are formed in this manner.

e) *Local Interstellar* H I *Densities*

In Paper I a rather low value was suggested for the average interstellar hydrogen density between the Sun and α Boo. The density determination is complicated by the fact that the intrinsic Lα profile is not known, and is probably intrinsically self-reversed as in the solar case. Also, the present data for α Tau and β Gem are of substantially lower quality than those previously reported for α Boo.

In order to estimate n_H, the interstellar neutral hydrogen number density in the direction of β Gem, we have assumed an intrinsic stellar profile having the same shape as the solar Lα profile (Bruner and Rense 1969) but with no intrinsic self-reversal, a half-width equal to the value quoted in Table 2 for β Gem, and three different values of n_H (0.1, 0.05, and 0.025 cm^{-3}). In each case (Fig. 5) it was possible to reproduce the observed Lα emission by multiplying the intrinsic profile by a normalization factor, adjusting the assumed stellar line half-width by about 10 percent, and choosing an appropriate wavelength shift relative to the star for the interstellar absorption (+0.04 Å for $n_H = 0.1$ cm^{-3}, and +0.08 Å for $n_H = 0.05$ and 0.025 cm^{-3}).

The three intrinsic stellar profiles required to reproduce the observed stellar intensity are shown in Figure 5, along with the predicted intensities resulting from the three assumed densities. In each case the computed profiles have been degraded to a resolution of 0.4 Å in order to compare them with the data which are shown as a solid histogram. Zero line-of-sight velocity dispersion for the hydrogen was assumed. For this value of the resolution (0.4 Å) it is not possible to distinguish between zero and 10 km s^{-1} velocity dispersion.

The situation is also complicated because geocoronal emission contaminates the two spectral steps at line center and thus it is not possible to determine if the observed absorption is indeed saturated. The clear conclusion is that one cannot use these data to distinguish between different small values of the H I column density unless the signal-to-noise ratio is improved substantially and resolution sufficient to separate the geocoronal component and the stellar profile is used. Furthermore, there is no compelling reason why the Lα emission from β Gem should have the same shape as the solar Lα profile. Still, to allow an interstellar density as high as 0.15 cm^{-3}, it would be necessary to have an intrinsic profile with steeper sides than the solar profile, and flared wings which the solar profile lacks; both seem very unlikely.

For α Tau the observed Lα profile is very asymmetrical (Fig. 1), and the absorption (or self-reversal) is very broad. Attempts to use the above procedure naturally result in less satisfactory fits to the data, leading to the conclusion that either the intrinsic stellar profile does not have the same shape as the solar Lα emission (with the self-reversal removed) or the absorption profile is not well characterized by low line-of-sight velocity dispersion (less than 10 km s^{-1}), or both. Nonetheless, an upper limit of 0.2 cm^{-3} for the hydrogen density between the Earth and α Tau can be deduced if one does arbitrarily make these assumptions despite the rather poor fit that results. Asymmetry is introduced in the computed profile by choosing an appropriate wavelength shift (relative to the star) for the Lα absorption center. For α Tau the best fits are obtained using shifts on the order of −0.16 Å (−40 km s^{-1}) to −0.20 Å (−50 km s^{-1}).

Although the data for α Tau and β Gem do not set strong limits on the local interstellar hydrogen density, it should still be possible to use late-type dwarf stars that are nearer to the Earth than these two giants to set an upper limit on the *local* H I density. The difficulty in using β Gem to measure the interstellar H I density is that the spectral data are so noisy that very low resolution is required to obtain a reasonable signal-to-noise ratio. Furthermore, the intrinsic stellar profile is too narrow to allow a star at a distance as great as 11 pc to be used to unambiguously determine the wings of the interstellar absorption. On the other hand, although the α Tau emission profile is probably broad enough to see the complete interstellar absorption wings, the problem with this late-type giant with low gravity is the possibility of circumstellar absorption (due to a large mass loss) which entwines the interstellar absorption with a circumstellar component. These problems can be overcome by observing nearby (less than 5 pc) K-type stars with surface gravities on the order of or larger than that of β Gem. The star ε Eri (K2 V), which has an observed Lα emission stronger than that from β Gem (our unpublished data) and is only 3.3 pc from the Sun, is an excellent candidate for use in determining the local interstellar H I density.

Analysis of the Lα sky background measurements from OGO-5 indicates an interstellar wind of neutral H I which penetrates the heliosphere (Bertaux *et al.* 1972). The direction ($\alpha = 263 \pm 5°$, $\delta = -17 \pm 5°$) of the incoming flow is determined directly from observation. Detailed models which best fit the observed distribution of sky background intensity require H I densities of 0.08–0.12 cm^{-3}, a streaming velocity of 2–9 km s^{-1}, and a temperature of 10^3 K to 1.4×10^4 K (cf. Thomas 1972; Fahr 1974).

Using this model, one may compute the component of the H I streaming velocity parallel to the direction of an observed star ($v_\parallel$) and predict the Doppler shift of the interstellar absorption component with respect to line center in the rest frame of the star. Since the *Copernicus* spectra are corrected for the stellar radial velocity v_r, the interstellar line displacement is $-(v_r - v_\parallel)$. Implicit in this procedure is the assumption that the interstellar medium is relatively homogeneous over the distance to the observed star. Table 3 summarizes the results of this procedure for four nearby stars.

The Doppler shifts and densities predicted from the Lα sky background measurements are consistent with the results obtained above for β Gem. The situation

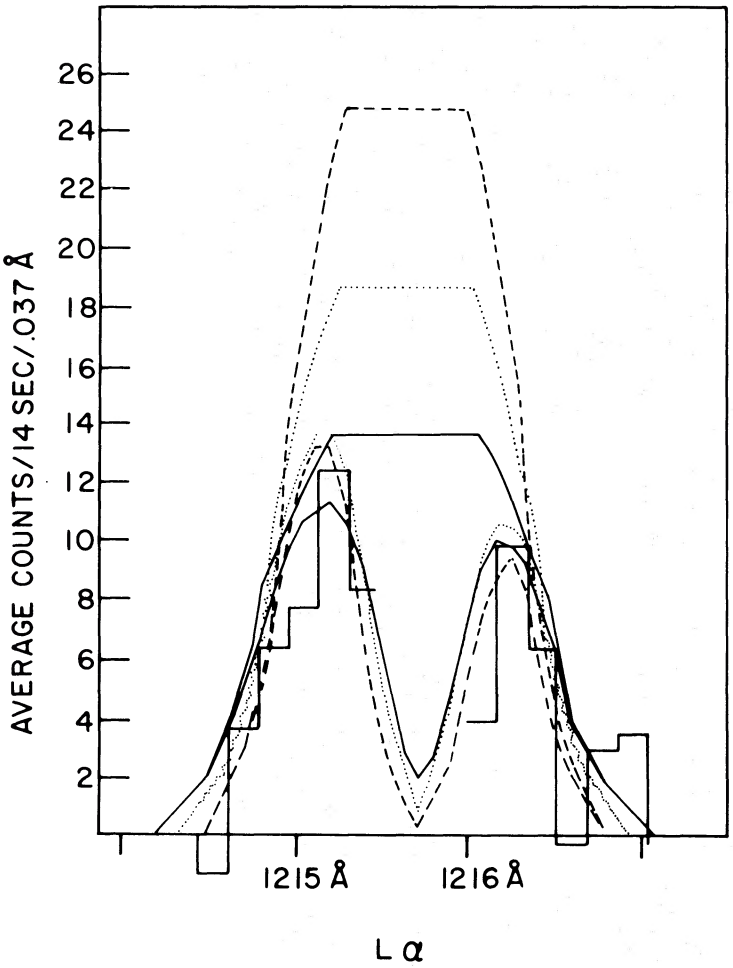

FIG. 5.—The β Gem Lα profile of Fig. 2 (*histogram*) is compared with three models for the intrinsic stellar Lα profile (*upper three curves*) and different amounts of interstellar absorption (*dashed line*, 0.1 cm^{-3}; *dotted line*, 0.05 cm^{-3}; *solid line*, 0.025 cm^{-3}). All three fit the data reasonably well.

for α Tau is complicated by the fact that the absorption profile is not easily fitted by a simple model of a symmetric intrinsic stellar line shape and a cloud of cool ($\lesssim 10^4$ K) H I, although the wavelength shift of the absorbing medium needed to most closely reproduce the observed profile is very close to the wavelength shift predicted from the sky background measurements. Thus one may not unambiguously estimate the relative extent to which interstellar absorption and stellar wind contribute to the observed asymmetry in the α Tau Lα profile.

The asymmetric absorption in the Lα profile of α Boo is not consistent with the sky background model. As for the case of α Tau, the absorption is not well modeled by a symmetric stellar profile and a cool absorbing cloud of H I ($T \lesssim 10^4$ K). Furthermore, the wavelength shift (about -0.25 Å, corresponding to a velocity of -60 km s^{-1}) of the absorbing medium relative to stellar line center is far different from the value $+0.01$ Å predicted from sky background measurements. Thus one must conclude either that the interstellar medium near the Sun in the direction of α Boo is very inhomogeneous over a distance of 10 pc or that some other physical process in the stellar chromosphere or in a shell surrounding the star is responsible for the high degree of asymmetry in the observed profile (cf. § III*f*).

In their theory of a two-component interstellar medium, Field *et al.* (1969) estimated that the intercloud medium (ICM) parameters are: temperature $T = 9000$ K and neutral hydrogen atom density $\langle n_{\rm H} \rangle = 0.2$ cm^{-3}. The largest sample of data relevant to this question are the 12 Å resolution OAO-2 Lα observations of 95 stars (Savage and Jenkins 1972; Jenkins and Savage 1974). In this sample $\langle n_{\rm H} \rangle = 0.25$ cm^{-3} for their nine stars closer than 140 pc, and $\langle n_{\rm H} \rangle = 0.17$ cm^{-3} for the subset of five stars with lowest $\langle n_{\rm H} \rangle$ and thus least likely to have a cloud in the line of sight. However, Savage and Panek (1974) have concluded from a study of the *stellar* Lα line in B stars that the OAO-2 interstellar survey results for *lightly reddened* B stars should be considered as only upper

TABLE 3

WAVELENGTH SHIFTS OF INTERSTELLAR MATTER RELATIVE TO STAR

Star	v_r (km s^{-1})	$v_\parallel$ (km s^{-1})	$v_r - v_\parallel$ (km s^{-1})	$\Delta\lambda$(1215) (Å)	$\Delta\lambda$(2800) (Å)
α Tau.....	+54.0	5.3 ± 3.4	48.7 ± 3.4	−0.20 ± 0.01	−0.46 ± 0.03
α Boo.....	− 5.2	−2.8 ± 1.8	−2.4 ± 1.8	+0.01 ± 0.01	+0.02 ± 0.02
β Gem.....	+ 3.0	4.7 ± 3.0	−1.7 ± 3.0	+0.01 ± 0.01	+0.02 ± 0.03
ϵ Eri.....	+15.4	4.2 ± 2.7	11.2 ± 2.7	−0.05 ± 0.01	−0.11 ± 0.03

limits due to contamination of the interstellar line by the stellar line. Bohlin's (1973) *Mariner-9* observations are of slightly higher spectral resolution, and from this sample of 10 stars $\langle n_H \rangle$ can be more unambiguously determined. Since the Bohlin estimates of $\langle n_H \rangle$ are typically 30 percent below the OAO-2 values, we might expect the $\langle n_H \rangle$ of the local ICM to be 0.12 cm^{-3}. Rogerson and York (1973) have derived $\langle n_H \rangle = 0.14$ cm^{-3} in the direction of β Cen using high-resolution *Copernicus* observations of the Lβ line to directly separate the stellar and interstellar components. Bohlin (1975) in his sample of 40 OB stars observed, also at high resolution, by *Copernicus* finds 15 stars for which $\langle n_H \rangle \leq 0.10$ cm^{-3} and two stars (β CMa at 213 pc and ϵ CMa at 179 pc) for which $\langle n_H \rangle \leq 0.01$ cm^{-3}.

Our Lα observations of β Gem and α Tau are consistent with measurements of both the Lα sky background and local ICM densities of $0.02 \text{ cm}^{-3} \leq \langle n_H \rangle \leq 0.15 \text{ cm}^{-3}$ for β Gem and $0.02 \text{ cm}^{-3} \leq \langle n_H \rangle \leq 0.20 \text{ cm}^{-3}$ for α Tau. The upper limits have been deduced from the fact that extreme assumptions about the shape of the intrinsic stellar profiles relative to the solar shape are required to reproduce the observations for larger values of $\langle n_H \rangle$ and therefore may not be as reliable as upper limits set from observations of early-type stars. The observations of α Boo are not consistent with Lα sky background measurements, and it has not been possible to reproduce the observed profile using a symmetric stellar emission profile and interstellar densities $0.02 \text{ cm}^{-3} \leq \langle n_H \rangle \leq 0.5 \text{ cm}^{-3}$ with densities greater than 0.1 cm^{-3} providing unsatisfactory fits for temperatures $T \lesssim 10^4$ K. In the solar Lα profile, intrinsic self-absorption near line center is relatively small.

For the three K-type giants under study, the electron pressures at the top of their chromospheres are smaller than in the Sun (see below), and therefore the surface value of the Lα source function will be smaller and the stellar Lα profiles more self-reversed. Thus the local interstellar hydrogen density could be substantially less than values quoted above, and $\langle n_H \rangle$ could be as low as 0.01 locally. Such a low density is of significance regarding the questions of interstellar pressure equilibrium and of the visibility of nearby stars at $\lambda < 912$ Å (Cruddace *et al.* 1974). The recent *Copernicus* observations of O VI λ1032 absorption in the direction of many near and distant bright stars has been interpreted by Jenkins and Meloy (1974) and by York (1974*b*) as indicating the existence of hot low-density interstellar regions with $n_H \leq 0.01$. Our observations are not inconsistent with the very local interstellar medium being such a low-density region.

f) *Interstellar* Mg II *Absorption*

The results of the determination of the Lα interstellar absorption can be used to estimate the amount of interstellar Mg II absorption in the observed profiles. Column densities along the line of sight can be estimated from the values of $\langle n_H \rangle$ derived in § III*e* and the result that the ratio of abundances of interstellar metals (such as Mg) to that of hydrogen appears to be smaller than the solar ratio by a factor of 10 (Rogerson *et al.* 1973*b*). Thus for β Gem and α Boo, column densities of approximately 1×10^{13} cm^{-2} are obtained for $\langle n_H \rangle = 0.1$ cm^{-3} and $\log [N(\text{Mg II})/N(\text{H I})] = -5.46$. This column density is consistent with the logarithmic average of the column densities toward the four stars studied by Rogerson *et al.* (1973*b*). For this column density and a line-of-sight velocity dispersion of 7 km s^{-1}, the equivalent width of the Mg II λ2795 interstellar absorption line is 0.21 Å. The shift in wavelength of the absorption center from stellar line center is found from Table 3 to be ±0.02 Å for both β Gem and α Boo. Therefore, for both of these stars the interstellar component is significant in only a single spectrum bin centered at λ2795.5. From detailed calculations of the absorption profile we find that for an assumed resolution of 0.5 Å the central step may have an observed intensity 40 percent deeper than the intrinsic stellar value and the two adjacent steps have about a 7 percent reduction due to interstellar absorption. The optical depth of the λ2802.7 line is reduced by a factor 2, resulting in an equivalent width of 0.15 Å and a reduction of 30 percent at the spectral step at line center. For α Tau the column density may be as much as a factor of 4 greater if $\langle n_H \rangle \approx 0.2$. However, since the absorption is saturated the equivalent width for Mg II λ2797.5 is only increased to a value of 0.32 Å. From Table 3 the estimated wavelength shift is −0.46 Å, or about 1.4 spectral steps. Thus for the two spectral steps shortward of the step centered at 2797.5 Å the observed intensity may be as much as 40 percent lower than the intrinsic stellar value. The equivalent width for λ2802.7 was computed to be 0.27 Å, and therefore reduction in intensities of the two spectral steps shortward of line center can be estimated to be about 25 percent.

For this analysis the line-of-sight velocity dispersion was estimated from the results of Rogerson *et al.* (1973*b*). The most conservative value (7 km s^{-1}) was

chosen in order to set stringent upper limits. This analysis cannot explain the obvious asymmetry in the Mg II profiles of α Boo. For α Boo the *predicted* absorption center is symmetric with respect to the stellar emission profile—contrary to observation. For α Tau the predicted interstellar absorption accounts for some but probably not all of the asymmetry.

Since the stellar radial velocity and local H I streaming data cannot explain the wavelength shift of the α Boo absorption features for Lα (-0.25 Å or -60 km s^{-1}) or for Mg II (-0.35 km s^{-1} or -38 km s^{-1}), we consider alternative explanations. Interstellar absorption lines have been observed interferometrically for the Ca II, Na I, and CH$^+$ λ4232 lines. Unfortunately neither α Boo nor any nearby stars have been observed. The stars ρ Leo, ζ Oph, η Leo, and 68 Her, which are 16°–46° away in galactic latitude, have been observed by Hobbs (1971, 1973) and by Marshall and Hobbs (1972). The stars ρ Leo ($l = 235°$, $b = +53°$) and α Leo ($l = 219°$, $b = +51°$), which are closest to α Boo ($l = 15°$, $b = +69°$) in galactic latitude, do not show strong interstellar features more negative than -11 km s^{-1} or weak features more negative than -19 km s^{-1}. The other two stars ζ Oph ($l = 6°$, $b = +23°$) and 68 Her ($l = 56°$, $b = +33°$) are closer in galactic latitude to α Boo and show fairly strong absorption features near -27 km s^{-1}. These data cannot be used to rule out the possibility of interstellar absorption of -38 km s^{-1} or -60 km s^{-1} in the direction of α Boo because (1) the stars are not in the same direction as α Boo, and (2) the observations typically do not extend to velocities more negative than -30 km s^{-1}. Nevertheless, the important interstellar velocities seen in the direction of these four stars do not appear in the Lα and Mg II profiles of α Boo. This argues against explaining the α Boo absorption features as interstellar.

An alternative way of considering whether the velocities of -38 or -60 km s^{-1} can be interstellar relates to the work of York (1975) in which the intercloud medium toward λ Sco ($l = 352°$, $b = -2°$) is studied in detail. Since this star is only 112 pc away compared to the four stars described above (170–760 pc), the velocity dispersion seen toward this star is a better measure of local interstellar velocities. York finds rms velocities along the line of sight no larger than 5.6 km s^{-1} and a maximum velocity range of 17 km s^{-1} for lines of different ionization potential including those presumably located in the H II region surrounding λ Sco itself. These data suggest that it is highly unlikely that there exist in the very local interstellar medium velocity features displaced -38 or -60 km s^{-1} with respect to the H I streaming motion measured near the Sun, and thus the observed very blueshifted α Boo absorption features are not interstellar.

Another possible explanation for these features is that they arise in a shell or circumstellar envelope surrounding α Boo. This we feel is most unlikely because circumstellar lines are narrow, they are not seen in the visual spectrum of normal stars earlier than M0 (Deutsch 1960), and none of the circumstellar lines observed by Deutsch (1956) in α Her are seen in the Griffin (1960) Arcturus atlas. As a result we feel that the asymmetries seen in the α Boo Lα and Mg II lines are intrinsic to the chromosphere of this star.

IV. TRANSITION REGION AND CORONA MODELS

a) Mg II *Line Intensities as Pressure Indicators*

In the Sun the basic structure above the photosphere, indicated by observations of quiet and active regions, is of a chromosphere with a slow temperature rise between the temperature minimum and the layer where $T \approx 8500$ K, then a steep transition region interrupted by one and possibly more narrow temperature plateaus, followed by a corona characterized by temperatures in excess of 10^6 K (Goldberg 1974; Noyes and Kalkofen 1970; Vernazza *et al.* 1973; Shine and Linsky 1974). Although the outer solar atmosphere is inhomogeneous, there are strong physical arguments involving the energy balance between nonradiative heating, radiative losses, and thermal conduction, as well as the temperature-dependence of the radiative energy losses (cf. Cox and Tucker 1969), which suggest that the above general picture is reasonable for most structures in the Sun and for late-type stars in general.

Since the Mg II resonance lines are collision-dominated, their intensities depend on the chromospheric electron density and to a lesser extent on details of the temperature structure just below the 8500 K layer in the "chromosphere." Ayres and Linsky (1975) have produced a grid of chromospheric models to explain the Arcturus Mg II and Ca II resonance line intensities. Their adopted model assumed a plane-parallel hydrostatic-equilibrium atmosphere, with the temperature structure derived from a partial redistribution analysis of the Ca II line wings and a complete redistribution analysis of the Ca II and Mg II emission line cores. They derive a mass column density $m_0 = 3 \times 10^{-5}$ g cm^{-2} in the 8500 K layer at the top of the chromosphere and a pressure $P_0 = m_0 g = 0.0015$ dyn cm^{-2} at this layer. For a fully ionized gas the reduced electron pressure is $P_e = n_e T = 5.4 \times 10^{12}$ K cm^{-3}. The corresponding pressures in the quiet Sun are much larger, 0.16 dyn cm^{-2} and 6×10^{14} K cm^{-3}, respectively (Dupree 1972; Vernazza *et al.* 1973).

In the picture of the chromosphere-corona transition region described above for the Sun, there is much less than a pressure scale-height between the top of the "chromosphere" and the base of the "corona." Thus the P_0 and P_e values for the top of the "chromosphere" deduced from the Mg II lines should be valid also for the transition region and base of the corona. We assume as in Paper II that the same is also a good approximation for the K giants presently being studied.

We can estimate mass column densities for β Gem and α Tau from the relationship between stellar surface flux in the k line, $f(k)$, and m_0 in Figure 8 of Ayres and Linsky (1975). We obtain

$$m_0 = 0.3\left[\frac{f(k)}{7.6 \times 10^7}\right]^{1.43} \text{g cm}^{-2}, \qquad (1)$$

where the factor 0.3 arises from the need to satisfy the observed K-line flux and to incorporate the increased mass column density of the temperature minimum resulting from the partial redistribution calculation of the K-line wings. Using equation (1) we obtain $m_0(\beta\ \mathrm{Gem}) = 8.8 \times 10^{-6}$ g cm^{-2} and $m_0(\alpha\ \mathrm{Tau}) = 3.7 \times 10^{-6}$ g cm^{-2}. In Paper II the observed O v λ1218 line flux was used to derive a minimum value of $P_0^2/g = 2.76 \times 10^{-7}$ on the assumption that the coronal temperature was such as to maximize the O v emission. With the slightly revised value of the O v flux in Table 2, $P_0^2/g = 2.5 \times 10^{-7}$, corresponding to $m_0 \geq 1.8 \times 10^{-5}$ g cm^{-2}. This value of m_0 is only a factor of 2 larger than that predicted by equation (1), indicative of the uncertainty in our estimates of m_0. We adopt $m_0(\beta\ \mathrm{Gem}) = 1.8 \times 10^{-5}$ g cm^{-2} and estimate errors in m_0 of $\pm$ factor of 2 for β Gem and α Boo and $\pm$ factor of 3 for α Tau. Included in Table 4 are various pressure-related quantities for the corona and transition region of the three stars including the product of the emission measure and coronal temperature, which is proportional to P_0^2/g. The emission measure is needed in computing the free-free emission in the radio and X-ray portions of the spectrum.

b) *Models*

Paper II presented a straightforward method for deriving the temperature-height relation of a stellar transition region, assuming that radiative losses balance the divergence in the conductive flux directed down from the corona. Since the radiative loss term (Cox and Tucker 1969) assumes all transitions to be optically thin, this approach cannot be applied at temperatures much less than 30,000 K as the hydrogen Lyman lines should then be optically thick. The temperature structure $T(z)$ for such models depends mainly on P_e, but also on the coronal temperature T_{cor}.

For optically thin lines excited by electron collisions, the stellar surfaces flux in ergs cm^{-2} s^{-1} in the line is given by

$$f = \tfrac{1}{2} h\nu \int n_e C_{lu} \left[\frac{N(\mathrm{ion})}{N(\mathrm{atom})}\right]\left[\frac{N(\mathrm{atom})}{N(\mathrm{H})}\right] N(\mathrm{H})\,dz\,, \quad (2)$$

where C_{lu} is the collisional excitation rate and the two terms in the integral are the ionization fraction and relative atomic abundance for the ion in question. The photon flux at Earth F_{E}' (in photons cm^{-2} s^{-1}) for a transition region line in a star of 1 $R_\odot$ at a distance of 10 pc is then

$$F_{\mathrm{E}}' = \left(\frac{R_\odot}{10\ \mathrm{pc}}\right)^2 \frac{n_e C_{lu}}{2}\left[\frac{N(\mathrm{atom})}{N(\mathrm{H})}\right] N(\mathrm{H}) \times \int \left[\frac{N(\mathrm{ion})}{N(\mathrm{atom})}\right]\left(\frac{dT}{dz}\right)^{-1} dT = a P_e^2 \left(\frac{dT}{dz}\right)^{-1}. \quad (3)$$

In Figure 6, F_{E}' is given for four transition-region lines as a function of T_{cor} and $P_e/P_e(\odot)$, where $P_e(\odot) = 6 \times 10^{14}$ (Dupree 1972). These fluxes are based on transition region models described above, ionization equilibria of Jordan (1969), abundances of Lambert (1968) and Lambert and Warner (1968), and collision rates of Gabriel and Jordan (1971) and Dupree (1972). To convert to photon fluxes at Earth F_{E} for a given star, one must multiply F_{E}' by a geometrical gain factor

$$G = \left(\frac{R_*}{R_\odot}\right)^2 \left(\frac{10\ \mathrm{pc}}{d}\right)^2 = \left(\frac{M_*}{M_\odot}\right)\left(\frac{g_\odot}{g_*}\right)\left(\frac{10\ \mathrm{pc}}{d}\right)^2. \quad (4)$$

Included in Table 4 are predicted photon fluxes at Earth for the estimated values of P_e in the three stars and for several values of T_{cor} assuming the lines are formed in a transition region. For α Boo we have assumed one-third solar abundances except for oxygen where we have taken 60 percent of the Lambert (1968) solar abundance (Mount *et al.* 1975). We note that the Si III λ1206 line is predicted to be at least an order of magnitude less bright than the observed upper limits. Also the predicted O v λ1218 line flux is a factor of 230 less bright for α Boo than the observed upper limit. The β Gem O v λ1218 line is about 60 times brighter than predicted, as noted in Paper II, suggesting that the line is formed elsewhere in the β Gem atmosphere.

It is also possible to compute the flux expected from a stellar corona. In Paper II the line flux from an assumed isothermal hydrostatic equilibrium corona about β Gem was computed. In this approximation we can derive from equation (2) a photon flux at Earth F_{E}' for a standard star as described above,

$$F_{\mathrm{E}}' = \left(\frac{R_\odot}{10\ \mathrm{pc}}\right)^2 \frac{C_{lu}}{2}\left[\frac{N(\mathrm{ion})}{N(\mathrm{atom})}\right]\left[\frac{N(\mathrm{atom})}{N(\mathrm{H})}\right]\int n_e N(\mathrm{H})\,dz = \frac{P_0^2}{g}\, b(T_{\mathrm{cor}})\,. \quad (5)$$

Since the collisional excitation rate C_{lu} can be written in terms of a collision strength $\bar{\Omega}$ and excitation energy E_0,

$$C_{lu} = 8.65 \times 10^{-6} \frac{\bar{\Omega}}{g_l T_{\mathrm{cor}}^{1/2}} \exp\left(-E_0/kT_{\mathrm{cor}}\right) \quad (6)$$

(Gabriel and Jordan 1971), the temperature-dependent factor in the photon flux expression is relatively simple:

$$b(T_{\mathrm{cor}}) = 1.81 \times 10^{16}\left[\frac{N(\mathrm{ion})}{N(\mathrm{el})}\right]\left[\frac{N(\mathrm{el})}{N(\mathrm{H})}\right] \times \frac{\bar{\Omega}}{g_l T_{\mathrm{cor}}^{3/2}} \exp\left(-E_0/kT_{\mathrm{cor}}\right). \quad (7)$$

In Table 5 the quantity $b(T_{\mathrm{cor}})$ is given for several lines as a function of T_{cor}. Predicted photon fluxes at Earth, F_{E}, for the three stars are given in Table 4 for the coronal temperature of maximum flux.

The observed β Gem O v flux is consistent with a coronal temperature near 260,000 K as described in Paper II. The 3 σ upper limit for the α Boo O v line

TABLE 4

A. Model Parameters and Line Photon Fluxes

Model Parameters	β Gem	α Boo	α Tau
$m_0 g$ (cm^{-2})	1.8(−5)	3.0(−5)	3.7(−6)
g (cm s^{-2})	800	50	63
$P_0 = m_0 g$ (dynes cm^{-2})	1.4(−2)	1.5(−3)	2.3(−4)
$P_e = n_e T$ (K cm^{-3})	5.1(13)	5.4(12)	8.4(11)
P_e/P_e ($\odot$)	8.5(−2)	9.0(−3)	1.4(−3)
P_0^2/g (cgs)	2.5(−7)	4.5(−8)	8.5(−10)
$(P_0^2/g)/(P_0^2/g)_\odot$	2.7(−1)	4.8(−2)	9.1(−4)
EM × T_{cor} (K cm^{-5})	2.8(32)	5.0(31)	9.4(29)
G (geometrical gain)	110	550	470

B. Predicted Transition Region Line Photon Fluxes at Earth F_E(ph cm^{-2} s^{-1})

Line	log (T_{cor})	β Gem	α Boo	α Tau
O VI λ1031	6.5	6.9(−3)	2.6(−3)	5.6(−4)
	5.5	2.2(−3)	2.3(−3)	1.2(−3)
O V λ1218	6.5	3.9(−3)	1.4(−3)	3.0(−4)
	5.5	1.4(−3)	3.9(−4)	7.4(−5)
N V λ1238	6.5, 5.5	2.2(−3)	4.3(−4)	1.7(−4)
Si III λ1206	6.5, 5.5	6.2(−3)	1.5(−3)	7.0(−4)
	4.5	7.8(−5)	1.5(−5)	6.6(−6)

C. Predicted Coronal Line Photon Fluxes at Earth F_E(ph cm^{-2} s^{-1})

Line	log (T_{cor})	β Gem	α Boo	α Tau
O VI λ1031	5.5	2.8(−1)	1.5(−1)	4.0(−3)
O V λ1218	5.4	2.5(−1)	1.3(−1)	3.6(−3)
N V λ1238	5.3	1.4(−1)	4.3(−2)	2.0(−3)
Si III λ1206	4.8	1.5(0)	4.7(−1)	2.2(−2)

is a factor of $2\frac{1}{2}$ larger than the predicted value for T_{cor} = 250,000 K. Given the factor of 2 uncertainty in m_0 and thus of 4 uncertainty in P_0^2/g and F_E(O V), the data are not inconsistent with an α Boo corona similar to that of β Gem. Additional data are needed to settle the question of whether the two stars have the same T_{cor}. The predicted Si III λ1206 coronal line photon fluxes at 63,000 K are factors of 6, 2.8, and 0.1 times the 3 σ upper limits for β Gem, α Boo, and α Tau. For β Gem and α Boo the predicted and observed upper limits would be equal at coronal temperatures of ~90,000 K and ~80,000 K. We therefore conclude on this basis only that the coronal temperature of β Gem is near 260,000 K, that T_{cor} for α Boo is hotter than 80,000 K and possibly similar to β Gem, and that T_{cor} for α Tau is presently unknown.

c) *Trends in the Transition Regions and Coronae of K Giants*

The surface flux in transition region and coronal lines depends on pressure- and temperature-dependent terms. For transition-region lines the pressure-dependent term is essentially P_e since $(dT/dz) \approx P_e$ in the models. For coronal lines the corresponding term is P_0^2/g. We note in Table 4 a systematic trend of decreasing P_e and P_0^2/g with later spectral type, which manifests itself in a generally weaker extreme-ultraviolet spectrum with later spectral type. It will be important to test the reality of these trends as more data become available.

We would further like to speculate concerning possible trends in the coronal temperatures of K giants. The coronal temperature affects the coronal spectrum mainly through changes in the ionization equilibrium, and can be studied by examining the flux ratio Lα/O V λ1218, which is 2.6 for β Gem. For α Boo and α Tau, the O V λ1218 upper limits of Table 2 give >15 and >10 for this ratio, respectively. The corresponding solar ratio is 750 (Table 2). This suggests that T_{cor} for α Boo and α Tau may differ considerably from ~3 × 10^5, with the Si III λ1206 data possibly suggesting that T_{cor} is hotter.

The stars α Boo and α Tau differ from β Gem in being somewhat cooler and about a factor of 10–20 lower in gravity. Few detailed coronal models have been computed for late-type stars, and even these could be grossly in error due to major uncertainties in generation, propagation, and dissipation of waves in the outer atmospheres of these stars. Ulmschneider (1967) finds a trend of increasing coronal temperature with decreasing gravity in late G and early K stars, and Kuperus (1965) finds a similar trend in his grid of models with 4400 K effective temperature. It seems reasonable to expect, therefore, that α Boo and α Tau

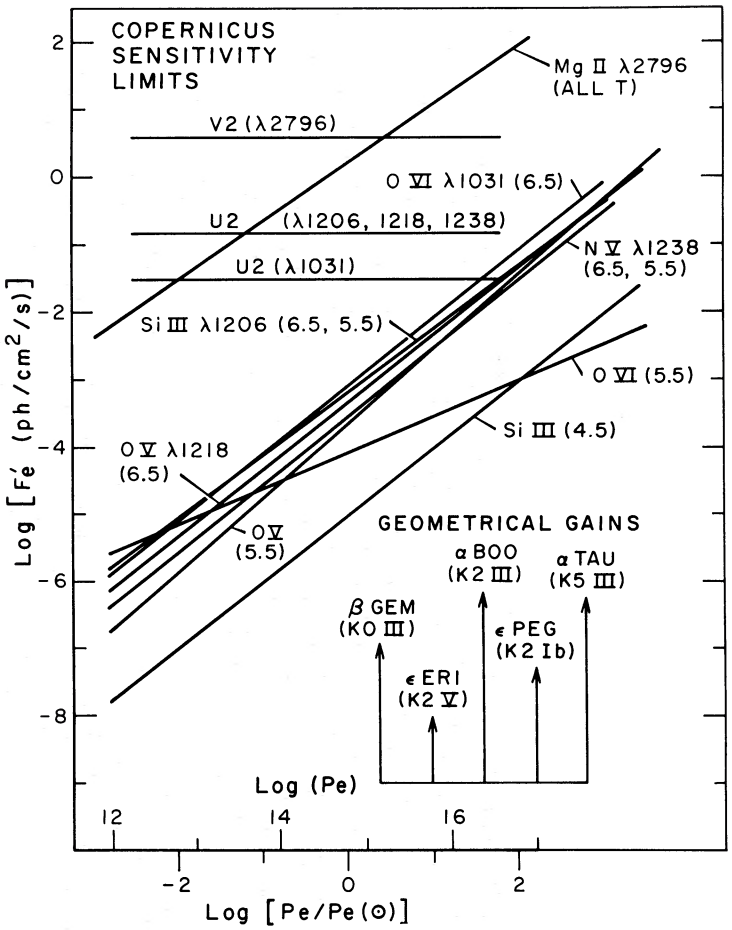

FIG. 6.—Estimates of the photon flux at Earth F_E' in ph cm^{-2} s^{-1} from the chromospheric line Mg II λ2796 and the transition region lines O VI λ1031, O V λ1218, N V λ1238, and Si III λ1206 from a standard K-type star of one solar radius and distance 10 pc. The photon fluxes are given as a function of electron pressure P_e and log (coronal temperature), the latter appearing in parentheses. To convert these fluxes to observed stellar fluxes, add the log of the geometrical gain factors $(R_*/R_\odot)^2/(d/10\text{ pc})^2$ to log F_E'. These factors for several stars are noted. Also given are the estimated 3 σ noise levels in the *Copernicus* V2 and U2 channels at the lines of interest for about 2 hours of scanning time.

TABLE 5

CORONAL REGION LINES

	Log [$b(T_{cor})$]			
	Si III λ1206	N V λ1238	O V λ1218	O VI λ1031
Log [T_{cor}] $\overline{\Omega}$	11.1	5.2	0.35	3.9
4.0.....	−1.947	...	...	...
4.2.....	2.006	...	...	...
4.4.....	3.762	...	...	...
4.6.....	4.553	...	...	...
4.8.....	4.743	...	...	...
5.0.....	3.536	1.585	1.301	...
5.2.....	1.487	3.582	3.241	1.280
5.4.....	...	3.239	3.950	3.611
5.6.....	...	2.152	2.995	3.770
5.8.....	...	1.292	1.043	2.647
6.0.....	...	0.907	−0.387	1.821
6.2.....	...	0.238	...	...

do not show O v emission because their coronae are far hotter than 3×10^5 K, rather than cooler.

V. SUMMARY

The important results of this paper are:

1. Asymmetries in the Mg II and Lα lines separate the stars into two groups. The stars α Boo and α Tau both show longward emission peaks in these lines far stronger than the shortward emission peaks if the latter are present at all. The asymmetry for α Boo is unlikely to be due to interstellar absorption but interstellar absorption may account for the α Tau asymmetries. This asymmetry for α Boo has been previously interpreted (Paper I) as indicating a stellar wind. The β Gem profiles, on the other hand, are more nearly symmetrical, suggesting a much weaker stellar wind.

2. There is a trend of increasing Lα line width with stellar luminosity. This trend may be similar to the Wilson-Bappu relation obtained for the Ca II lines. The Mg II profiles of all three stars are wider than the solar line profile, and also the α Tau and α Boo profiles may be wider at the base than the β Gem profile. This tends to confirm the line-width–luminosity correlation suggested by Kondo *et al.* (1972, 1975), Ayres *et al.* (1975), and Paper I, but the confirmation is weak because the data are so noisy.

3. The Lα and Mg II observations for α Tau show no clear time variation over a time scale of 8.3 months.

4. The Lα profiles are consistent with local interstellar hydrogen densities of less than 0.2 atoms cm^{-3} and possibly as low as 0.02 atoms cm^{-3}.

5. The intensities of the Mg II lines are useful indicators of the pressure in a stellar transition region and corona.

6. There is a trend of decreasing P_e and P_0^2/g with later spectral type and/or increasing stellar luminosity. Thus aside from considerations of the coronal temperature, the trend is toward a fainter spectrum from the transition region and corona in the sequence β Gem $\rightarrow \alpha$ Boo $\rightarrow \alpha$ Tau.

7. The O v λ1218 emission from β Gem is indicative of a corona in the neighborhood of 260,000 K, and the absence of observed α Boo and α Tau O v emission suggests that their coronae, if present, are hotter than 3×10^5 K.

This work was sponsored in part by the National Aeronautics and Space Administration through grants to the University of Colorado and to The Johns Hopkins University. The generous help of L. Spitzer in making available *Copernicus* observing time, and of D. G. York, T. P. Snow, and J. R. Rogerson in planning the observations, is gratefully acknowledged. We wish to also thank R. A. Shine and B. D. Savage for helpful suggestions.

REFERENCES

Ayres, T. R., and Linsky, J. L. 1973, *Bull. AAS*, **5**, 454.
———. 1975, *Ap. J.*, in press.
Ayres, T. R., Linsky, J. L., and Shine, R. A. 1974, *Ap. J.*, **192**, 93.
———. 1975, *Ap. J.* (*Letters*), **195**, L121.
Bertaux, J. L., Ammar, A., and Blamont, J. E. 1972, *Space Res.*, **11**, 1559.
Bohlin, R. C. 1973, *Ap. J.*, **182**, 139.
———. 1975, *Ap. J.*, in press.
Bruner, E. C. Jr., and Rense, W. A. 1969, *Ap. J.*, **157**, 417.
Chipman, E. 1974, private communication.
Conti, P. S., Greenstein, J. L., Spinrad, H., Wallerstein, G., and Vardya, M. S. 1967, *Ap. J.*, **148**, 105.
Cox, D. P., and Tucker, W. H. 1969, *Ap. J.*, **157**, 1157.
Cruddace, R., Paresce, F., Bowyer, S., and Lampton, M. 1974, *Ap. J.*, **187**, 497.
Deutsch, A. J. 1956, *Ap. J.*, **123**, 210.
———. 1960, in *Stellar Atmospheres*, ed. J. L. Greenstein (Chicago: University of Chicago Press).
———. 1970, in *Ultraviolet Stellar Spectra and Related Ground-Based Observations*, ed. L. Houziaux and H. E. Butler (Dordrecht: Reidel).
Doherty, L. R. 1972, *Ap. J.*, **178**, 495.
Dupree, A. K. 1972, *Ap. J.*, **178**, 527.
Evans, R. D. 1955, *The Atomic Nucleus* (New York: McGraw-Hill).
Fahr, H. J. 1974, *Space Sci. Rev.*, **15**, 483.
Field, G. B., Goldsmith, D. W., and Habing, H. J. 1969, *Ap. J.* (*Letters*), **155**, L149.
Gabriel, A. H., and Jordan, C. 1971, in *Case Studies in Atomic Collisional Physics*, ed. E. W. McDaniel and M. R. C. McDowell (Amsterdam: North Holland), chap. 4.
Gerola, H., Linsky, J. L., Shine, R., McClintock, W., Henry, R. C., and Moos, H. W. 1974, *Ap. J.* (*Letters*), **193**, L107 (Paper II).
Gezari, D. Y., Labeyrie, A., and Stachnik, R. V. 1972, *Ap. J.* (*Letters*), **173**, L1.
Goldberg, L. 1974, *Ap. J.*, **181**, 1.
Griffin, R. F. 1968, *A Photometric Atlas of the Spectrum of Arcturus* (Cambridge, England: Cambridge Philosophical Society).
Gustafsson, B., Kjaergaard, P., and Anderson, S. 1974, *Astr. and Ap.*, **34**, 99.
Hall, L. A., and Hinteregger, H. E. 1970, *J. Geophys. Res.*, **75**, 6959.
Hjellming, R. M., and Wade, C. M. 1971, *Ap. J.* (*Letters*), **168**, L115.
Hobbs, L. M. 1971, *Ap. J.*, **166**, 333.
Hobbs, L. M. 1973, *Ap. J.*, **181**, 79.
Hoffleit, D. 1964, *Catalogue of Bright Stars* (New Haven: Yale University Observatory).
Jenkins, E. B., and Meloy, D. A. 1974, *Ap. J.*, **193**, L121.
Jenkins, E. B., and Savage, B. D. 1974, *Ap. J.*, **187**, 243.
Johnson, H. L. 1964, *Bol. Obs. Tonantzintla y Tacubaya*, **3**, 305.
Jordan, C. 1969, *M.N.R.A.S.*, **142**, 501.
Joy, A. H. 1961*a*, *Ap. J.*, **133**, 493.
———. 1961*b*, in *Stellar Atmospheres*, ed. J. L. Greenstein (Chicago: University of Chicago Press), p. 563.
Kondo, Y. 1972, *Ap. J.*, **171**, 605.
Kondo, Y., Giuli, R. T., Modisette, J. L., and Rydgren, A. E. 1972, *Ap. J.*, **176**, 153.
Kondo, Y., Morgan, T. H., and Modisette, J. L. 1975, *Ap. J.* (*Letters*), **196**, L125.
Kuperus, M. 1965, *Res. Astr. Obs. Ultrecht*, **17**, 1.
Lambert, D. L. 1968, *M.N.R.A.S.*, **138**, 143.
Lambert, D. L., and Warner, B. 1968, *M.N.R.A.S.*, **138**, 213.
Liller, W. 1968, *Ap. J.*, **151**, 589.
Linsky, J. L., Basri, G., McClintock, W., Henry, R. C., and Moos, H. W. 1974, *Bull. AAS*, **6**, 458.
Marshall, L. A., and Hobbs, L. M. 1972, *Ap. J.*, **173**, 43.
McClintock, W., Linsky, J., Gerola, H., Shine, R., Henry, R. C., and Moos, H. W. 1974, *Bull. AAS*, **6**, 315.
McLaughlin, D. B. 1961, in *Stellar Atmospheres*, ed. J. L. Greenstein (Chicago: University of Chicago Press), p. 585.
Moos, H. W., Linsky, J. L., Henry, R. C., and McClintock, W. 1974, *Ap. J.* (*Letters*), **188**, L93 (Paper I).
Moos, H. W., and Rottman, G. J. 1972, *Ap. J.* (*Letters*), **174**, L73.

Mount, G. H., Ayres, T. R., and Linsky, J. L. 1975, *Ap. J.*, in press.
Noyes, R. W., and Kalkofen, W. 1970, *Solar Phys.*, **15**, 120.
Oster, L. 1971, *Ap. J.*, **169**, 57.
Pease, F. G. 1931, *Ergebn. Exakten Naturwiss.*, **10**, 84.
Rogerson, J. B., Spitzer, L., Drake, J. F., Dressler, K., Jenkins, E. B., Morton, D. C., and York, D. G. 1973*a*, *Ap. J.* (*Letters*), **181**, L97.
Rogerson, J. B., York, D. G., Drake, J. F., Jenkins, E. B., Morton, D. C., and Spitzer, L. 1973*b*, *Ap. J.* (*Letters*), **181**, L110.
Rogerson, J. B., and York, D. G. 1973, *Ap. J.* (*Letters*), **186**, L95.
Rottman, G. 1974, private communication.
Savage, B. D., and Jenkins, E. B. 1972, *Ap. J.*, **172**, 491.
Savage, B. D., and Panek, R. J. 1974, *Ap. J.*, **191**, 659.
Shine, R. A., and Linsky, J. L. 1974, *Solar Phys.*, **39**, 49.
Simon, T. 1970, Ph.D. thesis, Harvard University.
Snow, T. P. 1974, private communication.
Spencer, J. H., and Schwartz, P. R. 1974, *Ap. J.* (*Letters*), **188**, L105.
Thomas, G. E. 1972, NASA SP-308, 668.
Tousey, R. 1967, *Ap. J.*, **149**, 239.
Tousey, R., Milone, E. F., Purcell, J. D., Schneider, W., and Tilford, S. G. 1974, *An Atlas of the Solar Ultraviolet Spectrum between 2296 and 2992 Å* (NRL Report No. 7788).
Ulmschneider, P. 1967, *Zs. f. Ap.*, **67**, 193.
Vaughan, A. H., and Zirin, H. 1968, *Ap. J.*, **152**, 123.
Vernazza, J. E., Avrett, E. H., and Loeser, R. 1973, *Ap. J.*, **184**, 605.
Wade, C. M., and Hjellming, R. M. 1971, *Ap. J.* (*Letters*), **163**, L105.
Wesselink, A. J. 1969, *M.N.R.A.S.*, **144**, 297.
Wilson, O. C., and Bappu, M. K. V. 1957, *Ap. J.*, **125**, 661.
York, D. G. 1974*a*, private communication.
———. 1974*b*, *Ap. J.* (*Letters*), **193**, L127.
———. 1975, *ibid.*, **196**, L103.

W. McCLINTOCK, R. C. HENRY, and H. W. MOOS: Department of Physics, The Johns Hopkins University, Baltimore, MD 21218

JEFFREY L. LINSKY: Joint Institute for Laboratory Astrophysics, University of Colorado, Boulder, CO 80302

H. GEROLA: Physics Department, New York University, 4 Washington Place, New York, NY 10003